HEPATOLOGY

HEPATOLOGY, VOL. 68, NO. 6, 2018

Acetyl-CoA Carboxylase Inhibition Reverses NAFLD and Hepatic Insulin Resistance but Promotes Hypertriglyceridemia in Rodents

Leigh Goedeke,[1] Jamie Bates,[2] Daniel F. Vatner,[1] Rachel J. Perry,[1] Ting Wang,[2] Ricardo Ramirez,[2] Li Li,[2] Matthew W. Ellis,[3] Dongyan Zhang,[1] Kari E. Wong,[4] Carine Beysen,[5] Gary W. Cline,[1] Adrian S. Ray,[2] and Gerald I. Shulman[1,3,6*]

Pharmacologic inhibition of acetyl-CoA carboxylase (ACC) enzymes, ACC1 and ACC2, offers an attractive therapeutic strategy for nonalcoholic fatty liver disease (NAFLD) through simultaneous inhibition of fatty acid synthesis and stimulation of fatty acid oxidation. However, the effects of ACC inhibition on hepatic mitochondrial oxidation, anaplerosis, and ketogenesis *in vivo* are unknown. Here, we evaluated the effect of a liver-directed allosteric inhibitor of ACC1 and ACC2 (Compound 1) on these parameters, as well as glucose and lipid metabolism, in control and diet-induced rodent models of NAFLD. Oral administration of Compound 1 preferentially inhibited ACC enzymatic activity in the liver, reduced hepatic malonyl-CoA levels, and enhanced hepatic ketogenesis by 50%. Furthermore, administration for 6 days to high-fructose-fed rats resulted in a 20% reduction in hepatic *de novo* lipogenesis. Importantly, long-term treatment (21 days) significantly reduced high-fat sucrose diet–induced hepatic steatosis, protein kinase C epsilon activation, and hepatic insulin resistance. ACCi treatment was associated with a significant increase in plasma triglycerides (approximately 30% to 130%, depending on the length of fasting). ACCi-mediated hypertriglyceridemia could be attributed to approximately a 15% increase in hepatic very low-density lipoprotein production and approximately a 20% reduction in triglyceride clearance by lipoprotein lipase ($P \leq 0.05$). At the molecular level, these changes were associated with increases in liver X receptor/sterol response element-binding protein-1 and decreases in peroxisome proliferator–activated receptor-α target activation and could be reversed with fenofibrate co-treatment in a high-fat diet mouse model. *Conclusion:* Collectively, these studies warrant further investigation into the therapeutic utility of liver-directed ACC inhibition for the treatment of NAFLD and hepatic insulin resistance. (Hepatology 2018;68:2197-2211).

SEE EDITORIAL ON PAGE 2062

Nonalcoholic fatty liver disease (NAFLD) affects one in three Americans and is strongly associated with obesity, insulin resistance, type 2 diabetes (T2D), and cardiovascular disease.[1] NAFLD encompasses a spectrum of pathologies ranging from simple steatosis to nonalcoholic steatohepatitis (NASH) and is a key predisposing factor for the development of cirrhosis and hepatocellular carcinoma.[2] NAFLD develops when the rate of fatty acid input (fatty acid uptake and *de novo* synthesis with subsequent esterification to triglycerides) exceeds the rate of fatty acid output (fatty acid oxidation and secretion of very low-density

Abbreviations: ACC, acetyl-CoA carboxylase; βOHB, β-hydroxybutyrate; CPT1, carnitine palmitoyltransferase 1; DAG, diacylglycerol; DIO, diet-induced obesity; DKO, double knockout; DNL, de novo lipogenesis; EGP, endogenous glucose production; FFD, fast-food diet; GPAT1, glycerol-3-phosphate acyltransferase mitochondrial; HFSD, high-fat sucrose diet; HGP, hepatic glucose production; IRK, insulin receptor kinase; LCCoA, long-chain acyl-CoA; LPL, lipoprotein lipase; LXR, liver X receptor; NAFLD, nonalcoholic fatty liver disease; NASH, nonalcoholic steatohepatitis; NEFA, nonesterified fatty acid; PKC, protein kinase C; PPAR, peroxisome proliferator–activated receptor; PUFA, polyunsaturated fatty acid; SCD1, stearoyl-CoA desaturase 1; SD, Sprague-Dawley; SREBP1, sterol response element-binding protein; T2D, type 2 diabetes; V_{CS}, citrase synthase flux; VLDL, very low-density lipoprotein; and V_{PC}, pyruvate carboxylase flux.

Received December 23, 2017; accepted April 30, 2018.

Additional Supporting Information may be found at onlinelibrary.wiley.com/doi/10.1002/hep.30097/suppinfo.

Supported by the National Institutes of Health (P30 DK059635, R01 DK-040936, and R01 DK113984 to G.I.S. and F32 DK114954 to L.G.) and an investigator-initiated award from Gilead.

lipoprotein [VLDL]).[3] Genetic and physiological mechanisms regulating these processes have developed during evolution to cope with starvation but become dysregulated in the face of nutritional oversupply.[4] In this setting, they converge to promote the accumulation of ectopic lipids leading to the development of NAFLD and hepatic insulin resistance, which increases the risk of fasting hyperglycemia and T2D.[2] Although the direction of causality for this relationship remains uncertain,[5] numerous studies have demonstrated that hepatic accumulation of the lipid moiety, diacylglycerols (DAGs), leads to the activation of protein kinase C epsilon (PKCε) and impairment of hepatic insulin action.[6] In parallel, dysregulated adipose tissue lipolysis as well as intrahepatic lipolysis can drive hepatic gluconeogenesis by increasing fatty acid flux to the liver, hepatic acetyl-CoA levels, and pyruvate carboxylase activity.[7] Collectively, these processes promote hepatic insulin resistance and increased rates of hepatic glucose production (HGP) that promote fasting and postprandial hyperglycemia in T2D. Moreover, they suggest that therapies targeted to prevent hepatic lipid accumulation may be efficacious for treating NAFLD, insulin resistance, and T2D.

Acetyl-CoA carboxylase (ACC) catalyzes the adenosine triphosphate–dependent condensation of acetyl-CoA and carbonate to form malonyl-CoA and plays a crucial role in fatty acid metabolism.[8] In mammals, there are two isoforms of the ACC enzyme: ACC1, which is primarily expressed in lipogenic tissues (liver, adipose, lactating mammary gland), and ACC2, which is primarily expressed in oxidative tissues (heart, skeletal muscle).[8] ACC1 is located in the cytosol and is responsible for the rate-controlling and first committed reaction in *de novo* lipogenesis (DNL). In contrast, the mitochondrial membrane–embedded ACC2 negatively regulates fatty acid oxidation by producing localized malonyl-CoA, which allosterically inhibits carnitine palmitoyltransferase 1 (CPT1) and the transfer of long-chain CoAs into the mitochondria.[9]

The importance of ACC as a drug discovery target to lower liver triglycerides by simultaneously reducing fatty acid synthesis and stimulating fatty acid oxidation has been strongly supported by genetic and pharmacological studies.[10] Specifically, we demonstrated that reducing hepatic expression of ACC1 and ACC2 using antisense oligonucleotides results in marked reductions in hypertriglyceridemia, hepatic triglyceride content, and reversal of hepatic insulin resistance in a high-fat-fed rodent model of NAFLD and hepatic insulin resistance.[11] In addition, a liver-directed allosteric inhibitor of ACC1 and ACC2 (GS-0976) has been shown to improve hepatic steatosis and markers of liver injury in patients with NASH and to reduce hepatic steatosis and dyslipidemia in rodent models of obesity.[12-14] Despite this, the effect of liver-directed ACC inhibition on hepatic mitochondrial oxidation, anaplerosis, and ketogenesis

View this article online at wileyonlinelibrary.com.
DOI 10.1002/hep.30097

Potential conflict of interest: Dr. Bates, Dr. Ramirez, Dr. Wang, and Dr. Li own stock in Gilead. Dr. Beysen consults for Gilead. Dr. Shulman advises Novo Nordisk, Merck, and AstraZeneca; he received grants from Gilead.

ARTICLE INFORMATION:

From the [1]Department of Internal Medicine, Yale University School of Medicine, New Haven, CT; [2]Gilead Sciences Inc, Foster City, CA; [3]Department of Cellular and Molecular Physiology, Yale University School of Medicine, New Haven, CT; [4]Metabolon Inc., Morrisville, NC; [5]Independent Researcher, San Mateo, CA; [6]Howard Hughes Medical Institute, Yale University School of Medicine, New Haven, CT.

ADDRESS CORRESPONDENCE AND REPRINT REQUESTS TO:

Gerald I. Shulman, M.D., Ph.D.
Yale University School of Medicine
P.O. Box 208020, TAC S269
333 Cedar Street
New Haven, CT 06520-8020
E-mail: gerald.shulman@yale.edu
Tel: +1-203-785-5447

in vivo is unknown. Here, we performed a comprehensive set of metabolic flux analyses to assess these parameters in both chow-fed rats and rat models of diet-induced obesity (DIO). We hypothesized that chronic inhibition of hepatic ACC by Compound 1 (a liver-directed allosteric inhibitor of ACC) would lead to reduced hepatic fat content due to increases in hepatic mitochondrial oxidation and reduced DNL, which in turn would lead to increased hepatic insulin sensitivity. The data presented demonstrate that liver-directed inhibition of ACC significantly reduces hepatic steatosis and hepatic insulin resistance; however, long-term treatment was paradoxically associated with increased plasma triglycerides, consistent with a recent report on a prior clinical candidate.[15] As such, we also evaluated the effect of ACC inhibition on triglyceride metabolism and the effect of coadministration of a fibrate to understand the mechanism for this observation.

Materials and Methods

ANIMAL STUDIES

Male Sprague-Dawley (SD) rats were purchased from Charles River Laboratories. For high-fat diet supplemented with 1% sucrose drinking water (HFSD) studies, male SD rats were placed on a safflower oil–based high-fat diet (Dyets #112245) and supplemented with 1% (wt/vol) sucrose (Domino Foods Inc.) drinking water. Following 3 days of diet, rats were given 10 mg/kg body weight Compound 1 in approximately 200 mg of peanut butter (Skippy brand) or vehicle control once daily for 21 days. Unless otherwise stated, all rats were sacrificed by intravenous pentobarbital 2 to 6 hours following the last dose of Compound 1. Tissue samples were collected as described[7] and stored at −80 °C until subsequent analyses. All procedures were approved by the Institutional Animal Care and Use Committee of Yale University School of Medicine. Mouse studies were conducted at Covance Central Laboratories. C57BL/6 mice were administered either a standard chow diet (Harlan Teklad Global Diets 2014, TD2014) or a high-fat, high-cholesterol diet (Research Diets Inc., DB12079B), herein referred to as a fast-food diet (FFD)[16] for at least 5 months. Mice were administered fructose/glucose in drinking water. Compound 1 was dosed at 1 to 10 mg/kg/day PO. Fenofibrate (0.1%) was administered in chow *ad libitum* in the FFD.

METABOLIC FLUX AND HYPERINSULINEMIC-EUGLYCEMIC CLAMP STUDIES

Metabolic flux studies and clamp studies were performed as described[17] and in the Online Materials and Methods.

DNL STUDIES

Rats were fed a high-fructose (60%; Research Diets D02022704) diet and treated with 10 mg/kg body weight/day Compound 1 for 6 days. DNL was assessed according to established methods.[18]

PLASMA ANALYSIS AND LIPOPROTEIN MEASUREMENTS

The lipid distribution in plasma lipoprotein fractions and plasma metabolites was assessed as described[17,19] and in the Online Materials and Methods. β-hydroxybutyrate (βOHB) enrichment and endogenous glucose production (EGP) were measured by gas chromatography–mass spectrometry as described.[17] Hepatic mitochondrial fluxes were assessed by a combined ^{13}C nuclear magnetic resonance (NMR)/gas chromatography–mass spectrometry method using the positional isotopomer NMR tracer analysis as described.[20] Quantification of mouse plasma triglycerides and βOHB were performed by Metabolon.

HEPATIC VLDL SECRETION AND PLASMA LIPID CLEARANCE

Hepatic VLDL-triglyceride secretion and plasma lipid clearance were measured as described.[21] The lipoprotein lipase (LPL) activity was assessed in preheparin and postheparin plasma using the LPL Activity Assay Kit from Cell Biolabs Inc. according to the manufacturer's instructions.

HEPATIC LIPID ANALYSIS

Rat liver triglycerides, DAGs, ceramides, long-chain acyl-CoAs (LCCoAs), acylcarnitines, malonyl-CoA, and acetyl-CoA were extracted and

measured by liquid chromatography–tandem mass spectrometry as described.[17,22] Quantification of mouse hepatic triglycerides and cholesterol was performed by Metabolon Inc.

RNA ISOLATION, RNA SEQUENCING, REAL-TIME QUANTITATIVE PCR, AND WESTERN BLOT ANALYSIS

Hepatic RNA isolation and real-time quantitative PCR analysis were performed as described.[22] The real-time quantitative PCR analysis of lipid metabolism–related genes was performed using the Rat Lipid Metabolism Tier 1 and 2 Arrays (Bio-Rad) according to the manufacturer's instructions. RNA sequencing, western blot analysis, and PKCε translocation were performed as described[22] and in the Online Materials and Methods.

STATISTICS

Statistics were performed as described in the Online Materials and Methods.

Results

COMPOUND 1 TARGET ENGAGEMENT

To determine the potential of Compound 1 to exhibit *in vivo* efficacy, we measured ACC engagement and malonyl-CoA levels in the tissues of chow-fed male SD rats after acute treatment (1.5 hours) with 10 mg/kg Compound 1 (ACCi) or vehicle control. Compound 1 interacts within the dimerization site of the biotin carboxylase domain of ACC1 and ACC2 and specifically binds to the negative regulatory adenosine monophosphate–activated protein kinase phosphorylation site ($hACC1^{R172}$ and $hACC2^{R277}$) (Fig. 1A,B). By using a phospho-specific antibody that recognizes this site ($pACC^{S79}$), we found that acute treatment with ACCi significantly inhibited our ability to detect hepatic $pACC^{S79}$ (Fig. 1C), thereby confirming Compound 1 engagement of ACC. Consistent with this, ACCi treatment significantly reduced hepatic malonyl-CoA levels (Fig. 1D), whereas acetyl-CoA levels were unaffected (Supporting Fig. S1A-D). Importantly, no appreciable differences were detected in the phosphorylation status of ACC or malonyl-CoA levels in other metabolic tissues, including gastrocnemius (muscle), heart, epididymal white adipose tissue, and brain (Fig. 1C,D).

LIVER-DIRECTED INHIBITION OF ACC ENHANCES HEPATIC KETOGENESIS AND REDUCES HEPATIC LIPOGENESIS

To explore the functional consequence of inhibiting ACC1 and ACC2, we measured *in vivo* rates of hepatic mitochondrial oxidation, anaplerosis, ketogenesis, and lipogenesis in male SD rats. In accordance with ACCi-mediated reductions in hepatic malonyl-CoA content (Fig. 1D), acute treatment with 10 mg/kg ACCi significantly increased plasma βOHB and whole-body βOHB turnover compared with vehicle controls (Fig. 2A,B). Although no significant differences were observed in whole-body glucose turnover or fasting (~6 hours) plasma glucose (Supporting Fig. S2A-C), acute ACCi treatment significantly reduced plasma nonesterified fatty acids (NEFAs), most likely due to increased hepatic fat oxidation (Supporting Fig. S2G). Plasma insulin, total cholesterol, and triglycerides were similar between treatment groups (Supporting Fig. S2D-F).

We recently developed a positional isotopomer NMR tracer analysis method to measure changes in hepatic mitochondrial flux rates in awake rodents using [3-^{13}C]lactate and [1,2,3,4,5,6,6-$^{2}H_7$]glucose tracers.[20] Using this approach, we examined rates of hepatic pyruvate carboxylase flux (V_{PC}) and citrate synthase flux (V_{CS}) in awake, overnight-fasted chow-fed rats after an intragastric bolus of 10 mg/kg ACCi or vehicle control. In agreement with the results obtained from the approximately 6-hour-fasted rats, no significant differences were detected in EGP or rates of hepatic mitochondrial oxidative (V_{CS}) and gluconeogenic fluxes from pyruvate carboxylase (V_{PC}) (Fig. 2C-E; Supporting Fig. S2H-J).

We next ascertained the physiological significance of inhibiting ACC1. To this end, hepatic DNL was assessed using deuterated water in high-fructose-fed rats treated with ACCi or vehicle control ([10 mg/kg/day] × 6 days). Consistent with other reports,[15,23] ACCi treatment markedly reduced hepatic DNL and triglyceride content in a time-dependent manner by 23% to 36% and 43% to 61%,

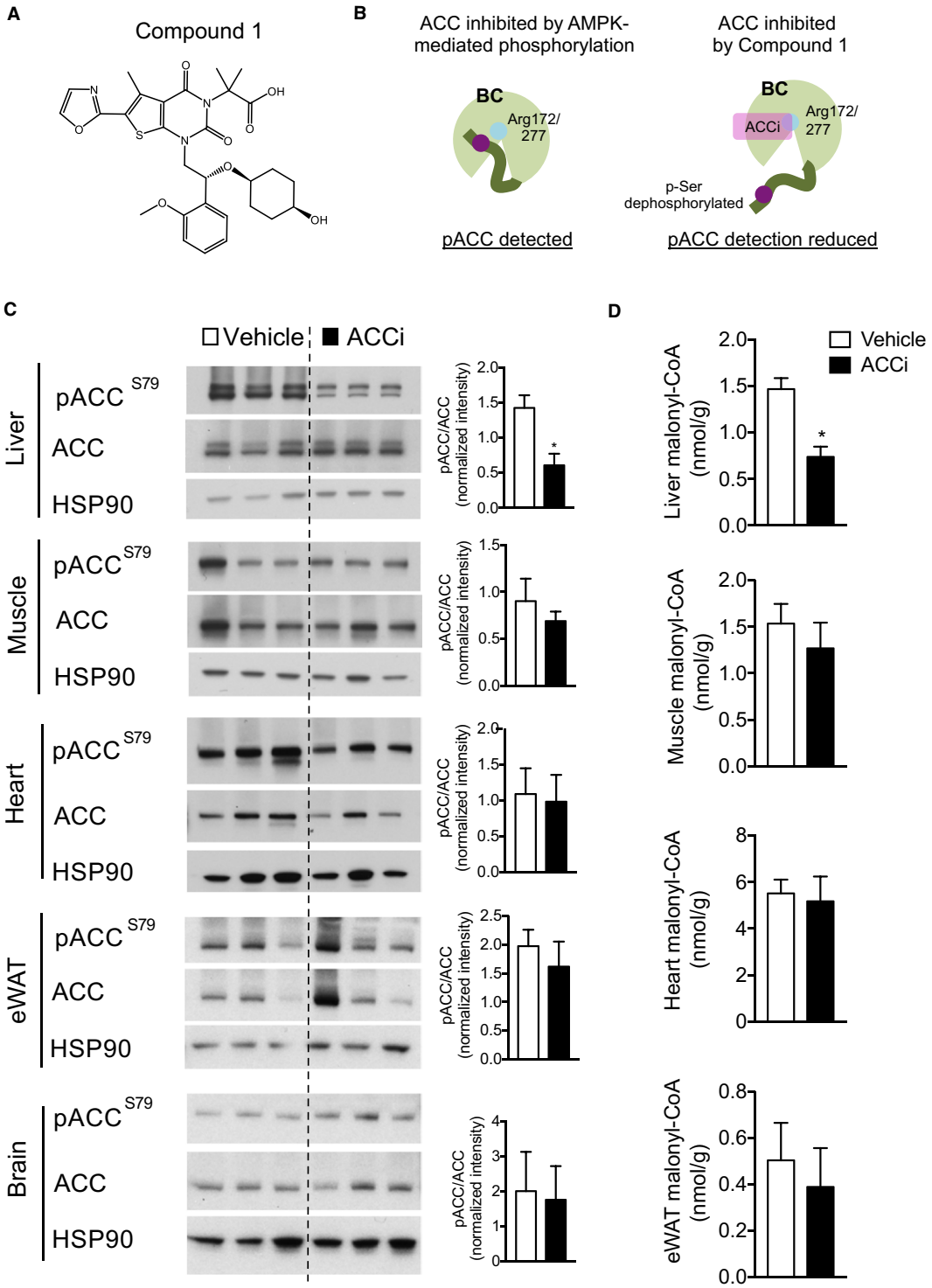

FIG. 1. Liver-directed inhibition of ACC by Compound 1. (A) Chemical structure of Compound 1. (B) Diagram depicting the use of adenosine monophosphate–activated protein kinase phosphorylation sites as a biomarker of ACC engagement by Compound 1. (C,D) Representative western blots depicting pACC (S79) and total ACC (C) and malonyl-CoA (D) in the liver, gastrocnemius muscle (muscle), heart, epididymal white adipose, and brain of chow-fed male SD rats treated with an intragastric bolus of 10 mg/kg Compound 1 (ACCi) or vehicle control for 1.5 hours. HSP90 was used as a loading control. Quantification of blots shown on the right. Data are presented as mean ± SEM. n = 6 to 9 per treatment group. $^*P \leq 0.05$ by unpaired Student t test compared with vehicle control. Abbreviations: EGP, endogenous glucose production; AMPK, adenosine monophosphate–activated protein kinase; BC, biotin carboxylase; eWAT, epididymal white adipose.

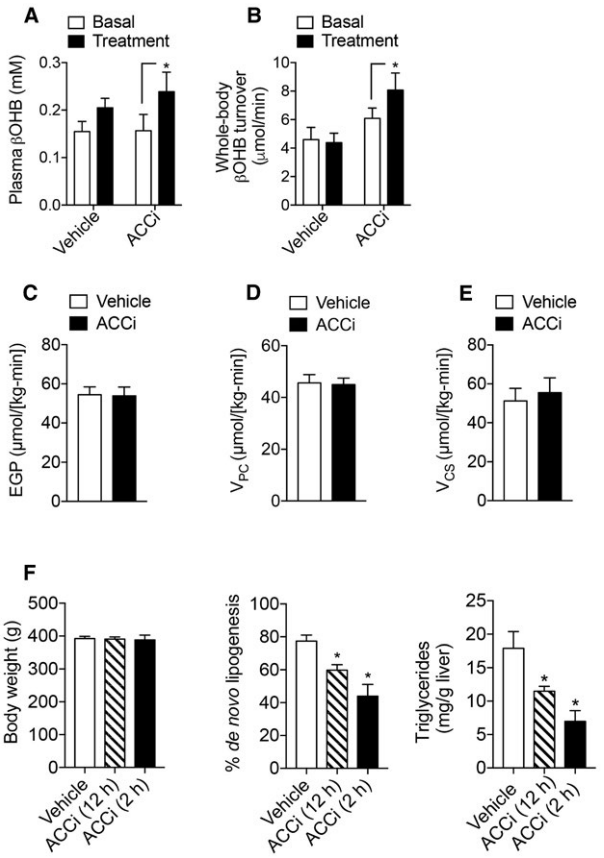

FIG. 2. Inhibition of ACC enhances hepatic ketogenesis and reduces hepatic DNL in chow-fed and high-fructose-fed rats, respectively. Plasma βOHB (A) and whole-body βOHB turnover (B) in chow-fed male SD rats fasted for 6 hours, infused with 0.1 mg/(kg-minute) [$^{13}C_4$]βOHB (basal) and treated with an intragastric bolus of 10 mg/kg Compound 1 (ACCi) or vehicle control for 1.5 hours (treatment). n = 6 to 9 per treatment group. Endogenous glucose production (EGP) (C), hepatic pyruvate carboxylase flux (V_{PC}) (D), and hepatic mitochondrial citrate flux (V_{CS}) (E) in male SD rats fasted overnight, infused with 0.1 mg/(kg-minute) [1,2,3,4,5,6,6-$^2H_7$]glucose and 40 μM/(kg-min) [3-^{13}C]lactate and treated as in (A). n = 7 per treatment group. (F) Body weight, percentage of DNL, and hepatic triglyceride content in male SD rats fed a high-fructose diet (60%) for 6 days and treated with ACCi (10 mg/kg/day) or vehicle control. Rates of DNL were assessed in the hepatic fatty acid pool after 3 days of treatment with deuterated water. Rats were sacrificed 12 hours (n = 12-14 per treatment group) or 2 hours (n = 6 per treatment group) after dosing. Data are presented as mean ± SEM. *$P \leq 0.05$ by paired Student *t* test compared with basal in each treatment group (A,B). *$P \leq 0.05$ by unpaired Student *t* test compared with vehicle control (C-F).

respectively (Fig. 2F). Collectively, these studies demonstrate the *in vivo* efficacy of ACCi to significantly reduce hepatic ACC activity, increase fatty acid oxidation, and reduce hepatic DNL.

LONG-TERM INHIBITION OF ACC REDUCES HEPATIC STEATOSIS BUT INCREASES FASTING PLASMA TRIGLYCERIDES AND NEFAS

To determine the long-term effect of ACC inhibition on glucose and lipid metabolism, male SD rats were fed an HFSD, a model that explores the ability of ACCi to reverse diet-induced NAFLD and insulin resistance by increasing fat oxidation and/or inhibiting DNL. To induce hepatic steatosis, rats were fed an HFSD for 3 days and then treated orally with 10 mg/kg/day ACCi or vehicle control for 21 days (Fig. 3A). This dose led to Compound 1 liver exposure of about 10 μM and inhibition of malonyl-CoA that approximated levels achieved clinically with GS-0976 (Fig. 3B,C). Importantly, Compound 1 muscle levels were close to the limit of quantitation (0.03 μM), thus further supporting the liver specificity of Compound 1 (Fig. 3B). Body weight, fasting plasma glucose, insulin, C-peptide, total cholesterol, and βOHB were similar between treatment groups, whereas plasma high-density lipoprotein (HDL) cholesterol was significantly increased in overnight-fasted ACCi-treated rats compared with controls (Table 1). Additionally, long-term inhibition of hepatic ACC did not alter plasma aminotransferases (Table 1). Importantly, ACCi prevented HFSD-induced hepatic steatosis, as observed both macroscopically and microscopically by hematoxylin and eosin and Oil Red O staining (Fig. 3D). Paradoxically, and consistent with human clinical data, long-term inhibition of ACC significantly increased plasma triglycerides by 30% to 130% (Table 1), despite an approximate 70% reduction in hepatic triglyceride content (Fig. 3E). Liver-directed inhibition of ACC also caused a 25% increase in fasting plasma NEFA concentration (Table 1).

LIVER-DIRECTED ACC INHIBITION IMPROVES HEPATIC INSULIN SENSITIVITY

Hepatic steatosis is strongly associated with hepatic insulin resistance, at least in part by DAG-mediated activation of PKCε and subsequent impairment of insulin receptor kinase (IRK) activity through increased phosphorylation of IRK threonine 1160 (murine threonine 1150).[22] Given the ability of long-term ACC inhibition to significantly reduce

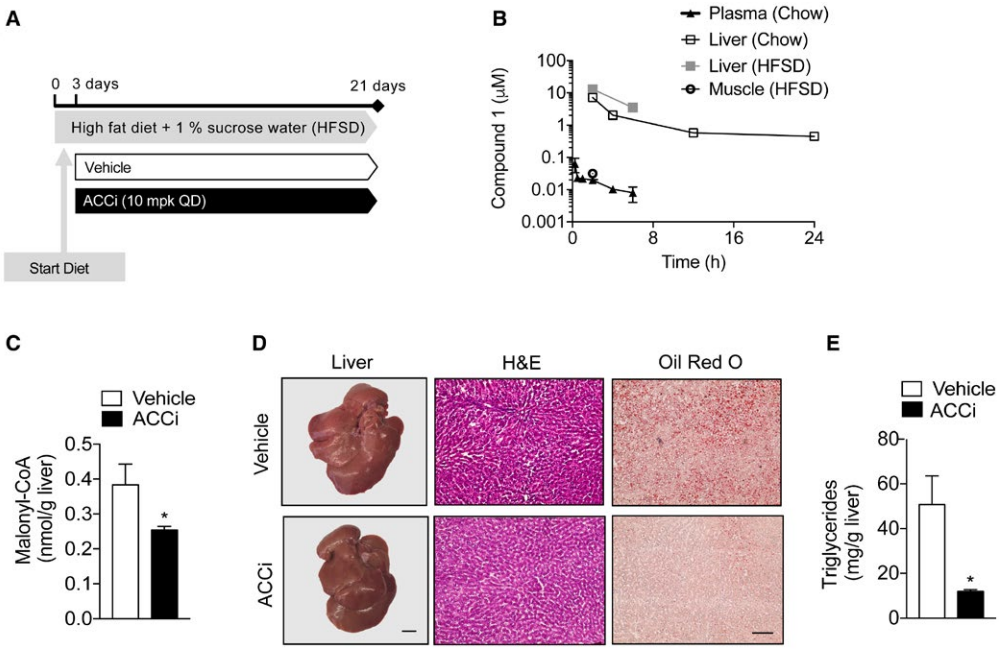

FIG. 3. Compound 1 reduces hepatic steatosis in high-fat diet fed rats. (A) Male SD rats were fed an HFSD (60% safflower oil supplemented with 1% sucrose drinking water) for 3 days and treated with 10 mg/kg/day Compound 1 (ACCi) or vehicle control for 21 days. (B) Plasma, liver, and muscle pharmacokinetics following single oral administration of 10 mg/kg Compound 1 to male SD rats fed a chow diet or rats treated as in (A) and treated with ACCi 2 hours or 6 hours before sacrifice (HFSD). n = 3 to 6 per treatment group. (C) Hepatic malonyl-CoA levels in overnight-fasted rats treated as in (A). (D) Representative livers (left) and liver sections stained with hematoxylin and eosin (middle) and Oil Red O (right) of overnight rats treated as in (A). Macroscopic scale bar = 6.4 mm; microscopic scale bar = 50 μm. (E) Hepatic triglyceride content in overnight-fasted rats treated as in (A). Data are presented as mean ± SEM. *$P \leq 0.05$ by unpaired Student t test compared with vehicle control. n = 5 per treatment group. Abbreviations: H&E, hematoxylin and eosin; QD, once daily.

TABLE 1. Metabolic Parameters

	6-Hour Fast		Overnight Fast	
	Vehicle	ACCi	Vehicle	ACCi
Physiologic parameters				
Body weight (g)	454.6 ± 10.9	421 ± 21.8	416 ± 16.5	409 ± 14.8
Plasma metabolites				
Glucose (mg/dL)	—	—	104.4 ± 4.7	105.3 ± 5.2
Insulin (μU/ml)	—	—	15.9 ± 3.0	19.3 ± 3.1
C-peptide (pmol/L)	—	—	366.4 ± 58.5	361.1 ± 67.5
Triglycerides (mg/dL)	122.5 ± 15.2	280.7 ± 35.7*	46.2 ± 4.1	61.7 ± 4.8*
Total cholesterol (mg/dL)	79.8 ± 5.1	69.3 ± 4.6	60.1 ± 1.9	64.4 ± 2.7
HDL-C (mg/dL)	31.75 ± 2.3	32.5 ± 2.0	16.0 ± 1.1	19.0 ± 1.0*
NEFAs (mM)	0.35 ± 0.1	0.45 ± 0.1	0.90 ± 0.05	1.13 ± 0.07*
βOHB (mM)	0.22 ± 0.6	0.20 ± 0.02	1.54 ± 1.4	1.40 ± 0.09
ALT (units/L)	30.6 ± 3.5	26.3 ± 0.93	30.2 ± 3.39	23.9 ± 0.28
AST (units/L)	81.3 ± 10.4	80.2 ± 9.0	105.2 ± 38.7	86.3 ± 11.1

Notes: Male SD rats were fed an HFSD for 3 days and treated with 10 mg/kg/day Compound 1 (ACCi) or vehicle control for 21 days. Data are presented as mean ± SEM; n = 8 to 9 per group (6-hour fast) or 11 to 12 per group (Overnight fast).
*$P \leq 0.05$ compared with vehicle-treated rats by unpaired Student t test. Abbreviations: HDL-C, high-density lipoprotein cholesterol; ALT, alanine aminotransferase; AST, aspartate aminotransferase.

hepatic triglycerides, we next assessed whole-body and tissue-specific insulin action in weight-matched HFSD-fed rats using hyperinsulinemia-euglycemic clamp studies (Supporting Fig. S3A). Oral administration of ACCi (10 mg/kg/day × 21 days) significantly reduced hepatic malonyl-CoA levels, whereas fasting plasma glucose concentrations were unchanged (Supporting Fig. S3B,C). Under hyperinsulinemic conditions, the glucose infusion rate required to maintain euglycemia was similar between treatment groups (Fig. 4A; Supporting Fig. S3D) and insulin-mediated whole-body glucose disposal was unchanged (Fig. 4B). However, ACCi treatment increased basal rates of hepatic glucose production (23%, $P \leq 0.05$), which could be attributed to a 14% increase in hepatic acetyl-CoA levels (Fig. 4D). In contrast, insulin-mediated suppression of EGP, indicative of hepatic insulin sensitivity, was significantly improved (Fig. 4E). Because adipose tissue lipolysis can indirectly alter hepatic gluconeogenesis, we next assessed plasma NEFA concentrations during the hyperinsulinemic-clamp. As shown in Fig. 4F and Supporting Fig. S3E, ACC inhibition did not significantly change plasma insulin levels or insulin-mediated suppression of circulating fatty acids, suggesting a direct hepatocellular effect for ACCi-mediated alterations in EGP.

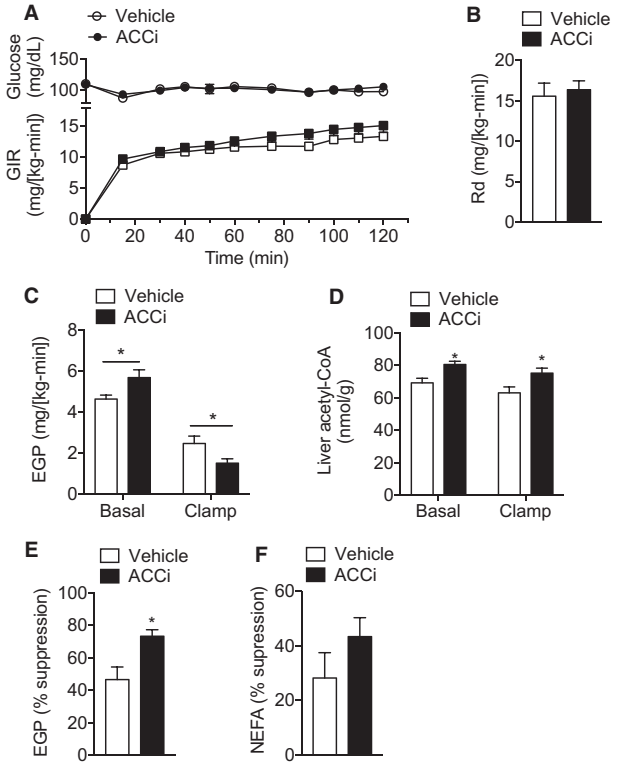

FIG. 4. Liver-directed inhibition of ACC improves hepatic insulin sensitivity. (A) Plasma glucose and glucose infusion rate during a hyperinsulinemic-euglycemic clamp (4 mU/[kg-minute]) insulin) in rats fed an HFSD for 3 days and treated with 10 mg/kg/day Compound 1 (ACCi) or vehicle control for 21 days (n = 10 per group). (B) Insulin-stimulated glucose disposal. (C) EGP during the basal and steady-state period of the clamp. (D) Hepatic acetyl-CoA levels in basal (overnight-fasted) and clamped rats treated as in (A). (E) Insulin-mediated suppression of EGP during the clamp. (F) Insulin-mediated suppression of plasma NEFAs during the clamp. In all panels, n = 10 per treatment group. Data are presented as mean ± SEM. *$P \leq 0.05$ by unpaired Student *t* test compared with vehicle control. Abbreviations: EGP, endogenous glucose production; GIR, glucose infusion rate; Rd, insulin-stimulated glucose disposal.

To understand the mechanism by which ACCi improved hepatic insulin sensitivity, we measured hepatic DAGs, ceramides, LCCoAs, acylcarnitines, and PKCε translocation in 6-hour-fasted HFSD-fed rats. Long-term inhibition of ACC resulted in a 27% reduction ($P \leq 0.05$) in hepatic DAG membrane content (Fig. 5A; Supporting Fig. S5A), whereas hepatic lipid and cytosolic DAG content, LCCoAs, and acylcarnitines were unchanged (Supporting Figs. S4 and S5B,C). The ACCi-mediated reduction in membrane DAGs was associated with a significant decrease in PKCε translocation to the plasma membrane and increased hepatic insulin action, as reflected by a 2-fold to 3-fold increase in insulin-stimulated AKT and IRK phosphorylation (Fig. 5C,D). Although total hepatic ceramide content was significantly decreased by ACCi treatment (Fig. 5B), two ceramide species implicated in resistance (C16 and C18 ceramides[24,25]) were not statistically different between treatment groups (Supporting Fig. S5D). Taken together, these data demonstrate that long-term inhibition of hepatic ACC reverses diet-induced NAFLD and hepatic insulin resistance by reducing DAG-mediated PKCε activation and improving hepatic insulin responsiveness.

INHIBITION OF HEPATIC ACC INCREASES VLDL SECRETION AND REDUCES LPL ACTIVITY

We next sought to define the mechanism responsible for the development of ACCi-mediated hypertriglyceridemia. To this end, we first measured plasma triglyceride concentrations in fast protein liquid chromatography–separated lipoprotein fractions from

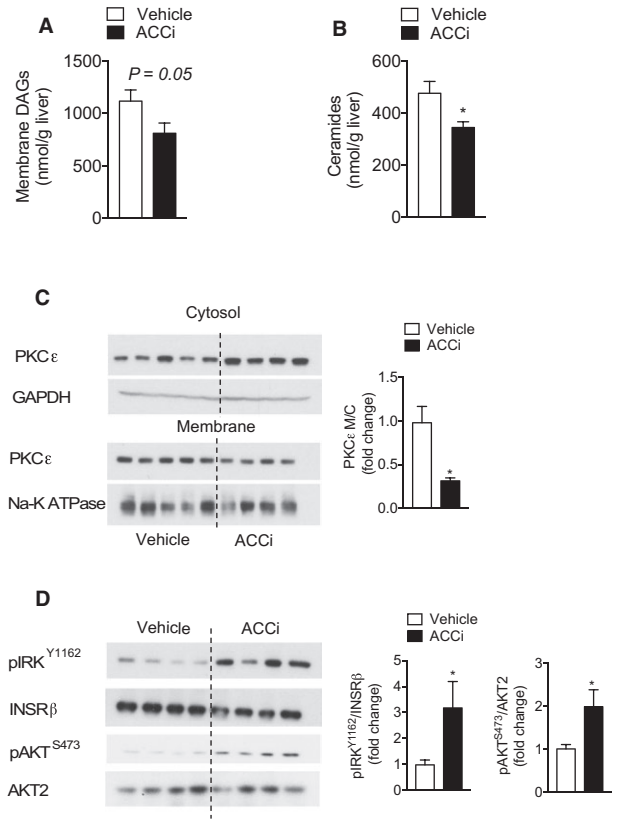

FIG. 5. Inhibition of hepatic ACC reduces membrane DAG content and PKCε translocation and increases hepatic insulin action in rats fed an HFSD. DAGs (A), total ceramides (B), and representative western blot of PKCε membrane to cytosol translocation (C) in the livers of 6-hour-fasted rats that were fed an HFSD for 3 days and treated with 10 mg/kg/day Compound 1 (ACCi) or vehicle control for 21 days. Glyceraldehyde 3-phosphate dehydrogenase and Na+/K+ ATPase were used as cytosolic and membrane loading controls, respectively. Quantification of blot shown in the right panel. (D) Representative western blot of pAKT^{S473}, AKT2, pIRK^{Y1162}, and INSRβ in clamped livers of rats treated as in (A). Quantification of blot shown to the right. n = 8 to 9 (A,C) or 12 to 13 (B) per treatment group. Data are presented as mean ± SEM. $^{*}P \leq 0.05$ by unpaired Student *t* test compared with vehicle control. Abbreviation: GAPDH, glyceraldehyde 3-phosphate dehydrogenase.

overnight-fasted HFSD-fed rats. Consistent with other reports, long-term inhibition of ACC primarily increased plasma triglycerides in the VLDL fraction (Fig. 6A,B). Hypertriglyceridemia may represent an increase in VLDL-triglyceride production that overcomes peripheral clearance and/or from a decrease in clearance without a compensatory decrease in production.[26] As such, we measured triglyceride secretion in overnight-fasted ACCi-treated rats after injection of Poloxamer 405 to inhibit lipolysis of triglyceride-rich lipoproteins.[27] Surprisingly, long-term inhibition of ACC significantly increased hepatic VLDL-triglyceride release by 15% (Fig. 6C,D), despite a marked reduction in hepatic DNL (Fig. 2F). As LPL-mediated triglyceride catabolism is another major determinant of circulating plasma triglycerides,[28] we also assessed plasma lipid clearance in ACCi-treated HFSD-fed rats after an intravenous bolus of Intralipid. Long-term inhibition of ACC was also associated with a significant reduction in lipid clearance by LPL (Fig. 6E,F).

DISEQUILIBRIUM OF NUCLEAR HORMONE RECEPTOR REGULATION IN ACCI-TREATED RATS

To ascertain the molecular mechanism by which long-term ACC inhibition leads to alterations in triglyceride production and clearance, we performed unbiased gene expression arrays in HFSD-fed rats treated with 10 mg/kg/day ACCi or vehicle control. These studies revealed that the mRNA levels of many genes regulated by the nuclear transcription factors liver X receptor α (LXRα) and sterol response element-binding protein (SREBP1c) (*Acc, Scd1* [stearoyl-CoA desaturase 1], *Pnpla3* [patatin-like phospholipase domain containing 3], and *Abca1* [ATP binding cassette transporter A1]) were significantly increased in the livers of ACCi-treated rats compared with controls (Supporting Fig. S6). In contrast, the mRNA levels of genes regulated by peroxisome proliferator–activated receptor (PPARα), including *Plin2, Fabp2,* and *Fabp4*, tended to be reduced (Supporting Fig. S6). Importantly, these findings were recapitulated at the mRNA level with independent primers and at the protein level by western blotting. Of note, long-term ACCi treatment significantly increased SREBP1 protein expression and the mRNA and protein levels of SREBP1c target genes,[29] including ACC, fatty acid synthase, SCD1, and glycerol-3-phosphate acyltransferase mitochondrial (GPAT1) (Fig. 6G-I). Consistent with this, liver-directed inhibition of ACC also significantly increased the hepatic 18:1/18:0 ratio, an indirect marker of SCD1 activity (Supporting Fig. S4A). In contrast, ACCi treatment did not alter the protein expression of other genes

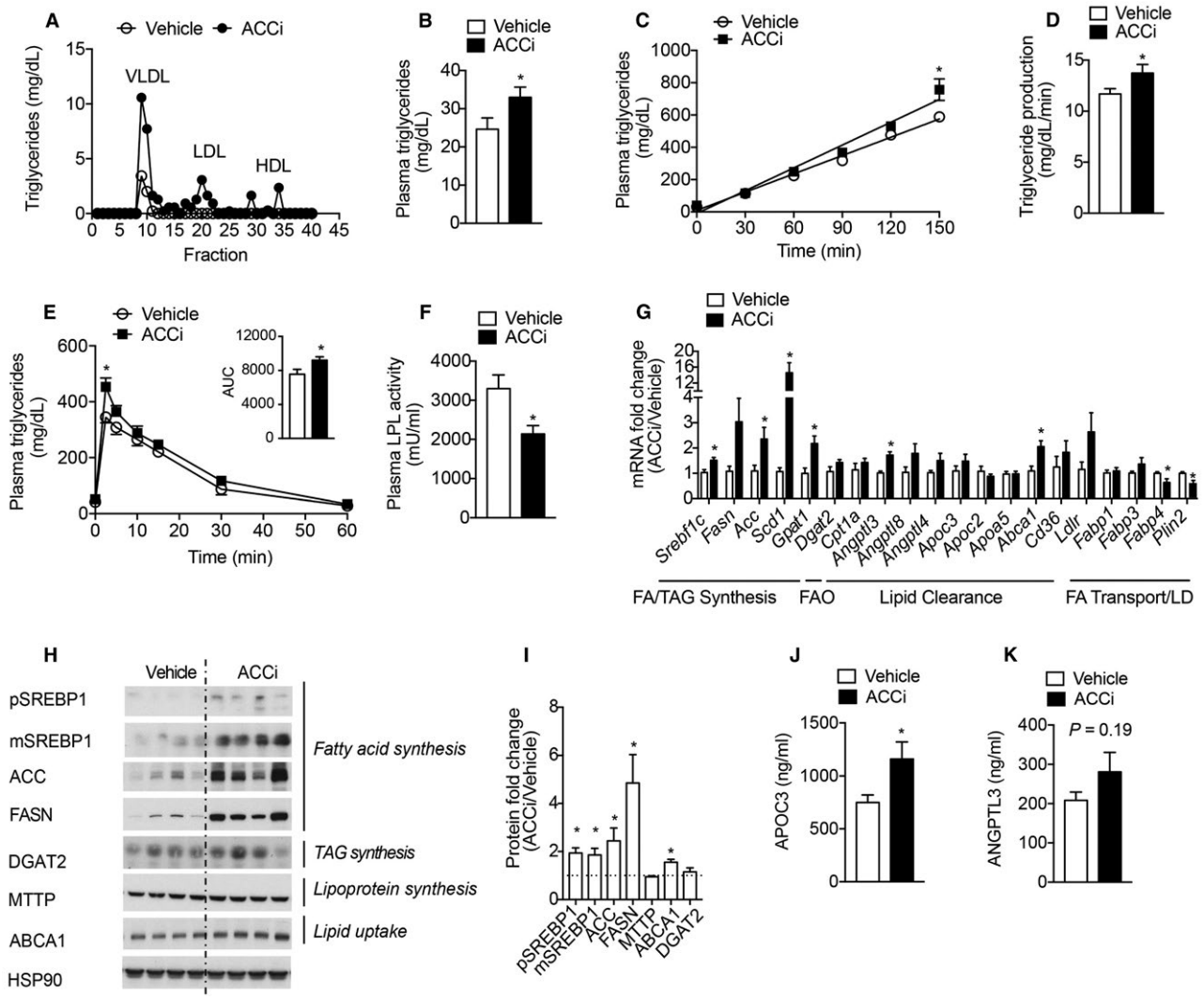

FIG. 6. Long-term inhibition of ACC increases hepatic triglyceride secretion and reduces plasma lipid clearance in HFSD-fed rats. (A) Plasma triglyceride content of fast protein liquid chromatography–fractionated lipoproteins from pooled plasma (n = 4 per group) of overnight-fasted rats that were fed an HFSD for 3 days and treated with 10 mg/kg/day Compound 1 (ACCi) or vehicle control for 21 days. (B) Fasting plasma triglycerides in rats treated as in (A). n = 12 per group. (C,D) Hepatic triglyceride production in overnight-fasted rats treated as in (A) and injected with Poloxamer 407 to inhibit lipolysis of triglyceride-rich lipoproteins. n = 10 to 14 per treatment group. (E) Lipid clearance test in overnight-fasted rats treated as in (A) and given an intravenous bolus of 20% Intralipid conjugated with ^{3}H-labeled triolein. n = 6 per treatment group. (F) Postheparin plasma LPL activity in rats treated as in (A). n = 7 to 9 per treatment group. mRNA (G) and protein (H) expression of indicated genes in the livers of overnight-fasted rats treated as in (A). n = 7 to 10 per treatment group. (H) HSP90 was used as a loading control. (I) Quantification of blot. (J) Plasma APOC3 concentration in rats treated as in (A). n = 7 per treatment group. (K) Plasma ANGPTL3 concentration in rats treated as in (A). n = 12 per treatment group. Data are presented as mean ± SEM. (B-G,J,K) *$P \leq 0.05$ by unpaired Student t test compared with vehicle control. Abbreviations: ANGPTL3, angiopoietin-like protein 3; AUC, area under the curve; FA, fatty acid; FAO, fatty acid oxidation; LD, lipid droplet; mSREBP1, mature SREBP1; pSREBP1, precursor SREBP1; TAG, triacylglycerol; TRL, triglyceride-rich lipoproteins.

(diacylglycerol o-acyltransferase 2 and microsomal triglyceride transfer protein) involved in triglyceride and lipoprotein synthesis, respectively (Fig. 6G-I). PPARα target genes also down-regulate the expression of the LPL inhibitor APOC3,[30] which showed a marked increase ($P \leq 0.05$) in the plasma of ACCi-treated rats compared with controls (Fig. 6J). Although angiopoietin-like protein 3, a negative

regulator of LPL activity and LXR target gene,[31] was significantly increased at the mRNA level (Fig. 6G), no significant differences were detected at the protein level (Fig. 6K). Additionally, ACC inhibition significantly increased hepatic ABCA1 expression (Fig. 7G-I), a key regulator of reverse cholesterol transport and plasma HDL cholesterol levels.[32] Collectively, this gene signature is consistent with other reports documenting a derepression of LXR/SREBP1 target genes caused by reduced levels of polyunsaturated fatty acids (PUFAs).[15,33] Given that ACCi markedly reduces hepatic malonyl-CoA levels (Fig. 3C), it is possible that this leads to a decrease in PUFAs and subsequent up-regulation of nuclear hormone signaling that ultimately drives increased VLDL-triglyceride secretion and reduced lipid clearance. Indeed, when we assessed PUFA levels in the triglyceride compartment of ACCi-treated livers, they were significantly reduced compared with controls (Supporting Fig. S7).

PPARα AGONISTS REVERSE THE PLASMA TRIGLYCERIDE INCREASE INDUCED BY ACCI

In a liver-specific ACC1 and 2 double knockout (ACC DKO) mouse,[15] the PPARα agonist WY14643 was shown to reduce elevated plasma triglycerides. Moreover, in patients with NASH who developed hypertriglyceridemia during treatment with GS-0976 in a phase 2 study, coadministration with fenofibrate led to reductions in plasma triglycerides.[13] Therefore, we tested the ability of fenofibrate dosed in chow concomitantly with ACCi to ameliorate the increase in plasma triglycerides observed with ACCi alone in an established murine model of NASH with enhanced DNL (Supporting Fig. S8A).

Mice were fed a diet high in fat, cholesterol, and fructose (FFD) for at least 5 months and treated with vehicle, ACCi (10 mg/kg once daily) or ACCi and fenofibrate (0.1% in chow) for 14 days. Substantial steatosis (approximately 20% steatotic area, with mean

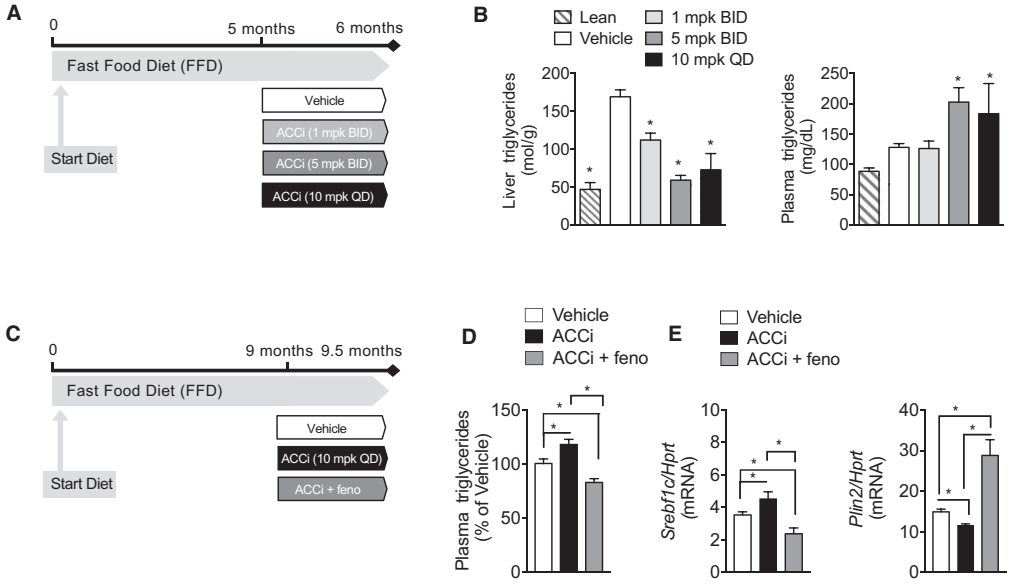

FIG. 7. Fenofibrate reverses ACCi-mediated hypertriglyceridemia in FFD-fed mice. (A) Male B6 mice were fed an FFD for 5 months and treated with 1 mg/kg (BID), 5 mg/kg (BID), 10 mg/kg (QD) Compound 1 (ACCi), or vehicle control for 28 days. (B) Liver and plasma triglycerides in mice treated as in (A). n = 8 to 13 per treatment group. (C) Male B6 mice were fed an FFD for 9 months and treated with vehicle, 10 mg/kg (QD) Compound 1 (ACCi), or 10 mg/kg ACCi (QD) and fenofibrate (0.1% in chow, feno) for 14 days. (D) Plasma triglycerides (pooled samples collected at 2, 6, and 24 hours following the dose) in mice treated as in (C). Values are expressed as percentage of vehicle-treated animals collected at the same time of day after treatment with vehicle, ACCi, or ACCi + fenofibrate. (E) mRNA expression of *Srebp1c* and *Plin2* (a canonical PPARα target) in the livers of mice treated as in (C). Data are presented as mean ± SEM. (B) $^*P \le 0.05$ compared with vehicle control by one-way analysis of variance with Dunnett correction for multiple comparisons. (D,E) $^*P \le 0.05$ by unpaired Student *t* test. Abbreviation: QD, once daily.

triglycerides >160 μmol/g or 35 mg/g) was observed in this long-term FFD model (Fig. 7A,B). In agreement with the data generated in HFSD-fed rats, 28 days of ACCi treatment in FFD-fed mice significantly increased plasma triglycerides and significantly lowered hepatic triglycerides, cholesterol, and PUFAs and reduced expression of a PPARα signature and increased SREBP1c and its target genes (Fig. 7A,B and Supporting Figs. S8B and S9A,B). After 2 weeks of dosing ACCi in this model, plasma triglycerides were significantly increased by 15% relative to vehicle-treated animals, whereas coadministration of fenofibrate in chow with ACCi significantly reduced plasma triglycerides relative to both the ACCi-treated group and the vehicle control group (Fig. 7C,D). Of note, these changes were associated with reversed alterations in PPARα/LXRα/SREBP1 gene expression (Fig. 7E and Supporting Fig. S10A-C), suggesting that LXRα/SREBP1 activation and PPARα reduction are required for ACCi-mediated hypertriglyceridemia. The addition of fenofibrate did not affect the ACCi-induced reduction of liver triglycerides but significantly further decreased liver cholesterol (Supporting Fig. S11A,B). In contrast to the 21-day treatment in rats fed an HFSD, plasma βOHB was significantly increased after 14 days of ACCi treatment in this mouse model (Supporting Fig. S11C). Moreover, addition of fenofibrate significantly increased βOHB relative to ACCi alone (Supporting Fig. S11C).

Discussion

Multiple studies support pharmacologic inhibition of ACC1 and ACC2 for the treatment of NAFLD through simultaneous inhibition of DNL and stimulation of fatty acid oxidation.[34] In particular, two clinical trials of the liver-directed ACC inhibitor GS-0976 found statistically significant decreases in hepatic steatosis and the marker of fibrosis tissue inhibitor of metalloproteinase 1 in patients with NASH and fibrosis.[12,13] However, the effect of ACC inhibition on hepatic mitochondrial oxidation, gluconeogenesis, hepatic glucose production, and ketogenesis *in vivo* has not yet been explored. Moreover, liver-directed inhibition of ACC has been associated with elevated plasma triglycerides in some patients.[15] To understand the mechanism for these observations, we examined the impact of Compound 1 on lipid and glucose metabolism in chow-fed rats and rodent models of DIO. Specifically, we demonstrate that acute treatment with Compound 1 significantly reduces hepatic ACC activity and malonyl-CoA levels in chow-fed rats. These results are in agreement with other studies and reflect the specific liver-targeted biodistribution of Compound 1 (Fig. 3B) due to its preferential uptake into hepatocytes through the organic anion-transporting polypeptide transporters.[23,35]

Malonyl-CoA is a substrate for DNL and inhibits the transport of fatty acids into the mitochondria through negative regulation of CPT1, leading to inhibition of fatty acid oxidation.[9] Consistent with Compound 1's ability to lower hepatic malonyl-CoA levels, liver-directed inhibition of hepatic ACC significantly increased plasma βOHB and βOHB turnover in chow-fed rats, indicative of increased fatty acid oxidation. Interestingly, the rise in plasma ketones was not detected after longer-term inhibition of ACC in overnight-fasted HFSD-fed rats. Given that hepatic malonyl-CoA levels are lower in the fasting state than in the fed state (approximately 0.4 nmol/g versus approximately 2 nmol/g), it is not surprising that ACCi had no further effect on fatty acid oxidation. Indeed, we have demonstrated that antisense oligonucleotide–induced reductions in ACC in high-fat-fed rats only led to detectable increases in plasma ketones in the fed state.[11] Accordingly, in FFD-fed mice (fasted for only 4 to 6 hours prior to sacrifice) plasma βOHB was significantly increased by ACCi, and the addition of fenofibrate increased βOHB relative to ACCi alone.

An important contributor to lipid accumulation in rodent models of NAFLD and patients with NAFLD is elevated rates of hepatic DNL.[36] Here, liver-directed inhibition of ACC in rats led to a significant reduction in hepatic DNL and triglycerides after only 1 week of high-fructose feeding. Longer-term inhibition of hepatic ACC also markedly reduced hepatic triglycerides in rats fed an HFSD and mice fed an FFD independent of changes in body weight, which was likely a combined effect of ACCi-mediated reductions in DNL and increases in fatty acid oxidation. The marked reduction in hepatic steatosis was associated with improved hepatic insulin sensitivity due to decreased hepatic DAGs and a reduction in PKCε activation in the liver. Although other lipid intermediates have been shown to trigger diet-induced insulin resistance, ACCi treatment

did not alter hepatic LCCoAs, acylcarnitines, or the ceramide species implicated in resistance (C16 and C18[24,25]). Collectively, these data are consistent with studies reporting an association with reductions in DAG-mediated PKCε activation and improved hepatic insulin responsiveness at the level of IRK.[2]

Despite the reduction in hepatic lipid accumulation and improved hepatic insulin sensitivity, as reflected by suppression of HGP during a hyperinsulinemic-euglycemic clamp, long-term ACC inhibition was associated with increases in rates of basal HGP in HFSD-fed rats. This increase was independent of changes in plasma insulin concentrations and likely reflects increases in hepatic acetyl-CoA content, which has been shown to increase hepatic gluconeogenesis through allosteric activation of pyruvate carboxylase.[7] The opposing effects of increased hepatic insulin sensitivity and increased HGP may explain the lack of an effect on fasting plasma glucose observed in this study and in patients with NASH treated for 12 weeks with GS-0976.[12,13] The net effect of these changes on long-term glycemic control in patients with metabolic dysfunction requires further clinical investigation.

In agreement with recent clinical data, allosteric inhibition of ACC by Compound 1 was also associated with a significant rise in plasma triglyceride levels, despite a marked reduction in hepatic steatosis.[12,13] These effects were mediated by a disequilibrium in nuclear receptor regulation due to a loss of hepatic malonyl-CoA, which is essential for the formation of PUFAs. n-3 and n-6 PUFAs act at the nuclear level to affect the expression of genes involved in lipogenesis and fatty acid oxidation.[33] Specifically, reduced SREBP1 activation by PUFAs has been proposed to be mediated by the inhibition of LXRα activity,[37,38] a potent inducer of SREBP1 transcription, or by direct inhibition of SREBP1 proteolytic maturation.[39] PUFAs also act as endogenous ligands for PPAR and have been shown to stimulate hepatic fatty acid catabolism through the activation of PPARα and CPT1. Here, we demonstrate that ACCi treatment significantly reduced PUFAs in the hepatic triglyceride compartment and induced the expression of multiple LXR/SREBP1 target genes in HFSD-fed rats and FFD-fed mice, which led to increased hepatic VLDL secretion (Supporting Fig. S12). This was somewhat surprising given the marked reduction of hepatic triglycerides observed in ACCi-treated animals. However, studies have shown that a large percentage of VLDL-triglycerides are derived from peripheral fatty acids and that GPAT1 plays an important role in channeling fatty acids into triglycerides for VLDL secretion.[36,40] Indeed, Kim et al[15] recently reported that increased hepatic expression of GPAT1 was necessary for the increased VLDL secretion and subsequent hypertriglyceridemia observed in liver-specific ACC DKO mice.

Although our data are consistent with studies documenting increased plasma triglycerides following ACC inhibition in humans and rodents,[15,41] there are several differences that warrant discussion. Studies generated from the Wakil laboratory were the first to report increased plasma triglycerides due to decreases in ACC activity. Specifically, they demonstrated that whole-body ACC2 KO mice fed a chow diet have a 30% increase in plasma triglyceride levels despite markedly lower hepatic triglycerides. Although the mechanism remains to be determined, it was postulated that the hypertriglyceridemia observed in ACC2 KO mice was due to the mobilization of triglycerides and fatty acids from peripheral organs to provide substrates for oxidation.[41] Given that Compound 1 is liver directed, it is unlikely that the rise in plasma triglycerides is due to mobilization of lipids from the periphery due to reduced malonyl-CoA; instead, the hypertriglyceridemia most likely results from a disequilibrium in hepatic nuclear receptor signaling pathways in an attempt to compensate for markedly low levels of hepatic DNL. Similar to observations by Kim et al., we demonstrate that ACC inhibition by Compound 1 results in an approximate 15% increase in VLDL secretion. However, we also report that liver-directed allosteric inhibition of ACC results in a 20% reduction in plasma LPL activity and corresponding decrease in triglyceride clearance. This is most likely a result of secreted factors that inhibit LPL activity, including PPARα-regulated APOC3. Although Kim et al. did not assess lipid clearance in their liver-directed ACC DKO mice, it is possible that reduced triglyceride catabolism also contributes to the rise in plasma triglycerides observed in their model.[15]

The degree of ACC inhibition could ultimately determine the mechanism(s) that drive hypertriglyceridemia in rodents and humans. In particular, a recent study reported that allosteric inhibition of ACC markedly reduced hepatic steatosis and increased insulin sensitivity, without altering plasma triglycerides in rat models of DIO.[23] MK-4074 (a

liver-directed inhibitor of ACC) was recently shown to increase plasma triglycerides in humans and mouse models of DIO.[15] ACC was completely inhibited by MK-4074 and in the liver-directed ACC DKO mice described by Kim et al.[15] Here, we used a dose of Compound 1 that better approximated the dose of GS-0976 (20 mg once daily) being assessed in human clinical trials. This may explain the different magnitudes of aberrant nuclear receptor signaling pathways and suggests that the mechanism for ACCi-mediated hypertriglyceridemia proposed in this study may be more relevant to ACC inhibitors that are currently under evaluation in clinical trials. Kim et al. showed that PUFA supplementation or the use of a PPARα agonist (WY14643) normalizes ACCi-mediated increases in plasma triglycerides.[15] Here, we demonstrate that coadministration of fenofibrate could ameliorate hypertriglyceridemia and stimulate fatty acid oxidation in FFD-fed mice.

In conclusion, the present study demonstrates that liver-directed allosteric inhibition of ACC significantly reduces hepatic malonyl-CoA levels, percentage of DNL, and hepatic triglycerides. Using stable isotope tracers, we also report that acute ACCi treatment significantly increases whole-body βOHB turnover in chow-fed rats, without altering whole-body glucose turnover or rates of hepatic mitochondrial citrate synthase flux (V_{CS}). Importantly, ACCi treatment markedly reduced HFSD-induced hepatic steatosis, which correlated with a significant reduction in hepatic DAGs, PKCε translocation, and improved hepatic insulin signaling at the level of the insulin receptor kinase. Steatosis reduction was also observed in mice on an FFD for 5 months. In rats, 21-day inhibition of ACC increased hepatic acetyl-CoA levels and HGP. Because this may serve to offset improvements in hepatic insulin sensitivity, it remains to be determined whether allosteric inhibition of hepatic ACC would have therapeutic benefit in treating fasting hyperglycemia in patients with NAFLD and T2DM. Moreover, ACCi treatment led to a significant rise in plasma triglycerides in HFSD-fed rats and FFD-fed mice. These effects were mediated by a reduction in hepatic PUFA levels and disequilibrium in nuclear hormone receptor expression that, in rats, resulted in increased hepatic VLDL secretion and reduced systemic triglyceride clearance. Although increased hypertriglyceridemia has been observed across species and in the clinic, preclinical and clinical data suggest that coadministration with a PPARα agonist can ameliorate hypertriglyceridemia induced by ACC inhibition.

Acknowledgments: We thank Jianying Dong, Mario Khan, Xian-Man Zhang, Sylvie Dufour, Irina Smolgovsky, Gina Butrico, John Stack, Yongliang Wang, Yuichi Nozaki, Codruta Todeasa, Maria Batsu, and the Yale Diabetes Research Core Facility for their expert technical assistance. We thank G. Mani Subramanian and Rob P. Myers for the helpful discussions. This study was designed by L.G., J.B., A.S.R., and G.I.S. Experiments were performed by L.G., D.F.V., J.B., R.J.P., T.W., R.R., L.L., K.E.W., C.B., M.W.E., and D.Z. Data were analyzed and interpreted by L.G., D.F.V., J.B., R.R., L.L., R.J.P., K.E.W., C.B., T.W., G.W.C., A.S.R., and G.I.S. The manuscript was written by L.G., J.B., A.S.R., and G.I.S., with input from all authors.

REFERENCES

1) Browning JD, Szczepaniak LS, Dobbins R, Nuremberg P, Horton JD, Cohen JC, et al. Prevalence of hepatic steatosis in an urban population in the United States: impact of ethnicity. Hepatology 2004;40:1387-1395.
2) Shulman GI. Ectopic fat in insulin resistance, dyslipidemia, and cardiometabolic disease. N Engl J Med 2014;371:1131-1141.
3) Fabbrini E, Sullivan S, Klein S. Obesity and nonalcoholic fatty liver disease: biochemical, metabolic, and clinical implications. Hepatology 2010;51:679-689.
4) Birkenfeld AL, Shulman GI. Nonalcoholic fatty liver disease, hepatic insulin resistance, and type 2 diabetes. Hepatology 2014;59:713-723.
5) Farese RV Jr, Zechner R, Newgard CB, Walther TC. The problem of establishing relationships between hepatic steatosis and hepatic insulin resistance. Cell Metab 2012;15:570-573.
6) Petersen MC, Vatner DF, Shulman GI. Regulation of hepatic glucose metabolism in health and disease. Nat Rev Endocrinol 2017;13:572-587.
7) Perry RJ, Camporez JP, Kursawe R, Titchenell PM, Zhang D, Perry CJ, et al. Hepatic acetyl CoA links adipose tissue inflammation to hepatic insulin resistance and type 2 diabetes. Cell 2015;160:745-758.
8) Brownsey RW, Zhande R, Boone AN. Isoforms of acetyl-CoA carboxylase: structures, regulatory properties and metabolic functions. Biochem Soc Trans 1997;25:1232-1238.
9) McGarry JD, Mannaerts GP, Foster DW. A possible role for malonyl-CoA in the regulation of hepatic fatty acid oxidation and ketogenesis. JClin Invest 1977;60:265-270.
10) Tong L, Harwood HJ Jr. Acetyl-coenzyme A carboxylases: versatile targets for drug discovery. JCell Biochem 2006;99:1476-1488.
11) Savage DB, Choi CS, Samuel VT, Liu ZX, Zhang D, Wang A, et al. Reversal of diet-induced hepatic steatosis and hepatic insulin resistance by antisense oligonucleotide inhibitors of acetyl-CoA carboxylases 1 and 2. JClin Invest 2006;116:817-824.
12) Lawitz EJ, Poordad F, Coste A, Loo N, Djedjos CS, McColgan B, et al. Acetyl-CoA carboxylase (ACC) inhibitor GS-0976 leads to suppression of hepatic de novo lipogenesis and significant improvements in MRI-PDFF, MRE, and markers of fibrosis

after 12 weeks of therapy in patients with NASH. JHepatol 2017;66:S34-S34.
13) Loomba R, Kayali Z, Noureddin M, Ruane P, Lawitz EJ, Bennett M, Wang L, et al. GS-0976 Reduces Hepatic Steatosis and Fibrosis Markers in Patients with Nonalcoholic Fatty Liver Disease. Gastroenterology 2018.
14) Stiede K, Miao W, Blanchette HS, Beysen C, Harriman G, Harwood HJ Jr, et al. Acetyl-coenzyme A carboxylase inhibition reduces de novo lipogenesis in overweight male subjects: A randomized, double-blind, crossover study. Hepatology 2017;66:324-334.
15) Kim CW, Addy C, Kusunoki J, Anderson NN, Deja S, Fu X, et al. Acetyl CoA carboxylase inhibition reduces hepatic steatosis but elevates plasma triglycerides in mice and humans: A bedside to bench investigation. Cell Metab 2017;26:576.
16) Charlton M, Krishnan A, Viker K, Sanderson S, Cazanave S, McConico A, et al. Fast food diet mouse: novel small animal model of NASH with ballooning, progressive fibrosis, and high physiological fidelity to the human condition. Am J Physiol Gastrointest Liver Physiol 2011;301:G825-G834.
17) Perry RJ, Peng L, Cline GW, Petersen KF, Shulman GI. A non-invasive method to assess hepatic acetyl-CoA in vivo. Cell Metab 2017;25:749-756.
18) Vatner DF, Majumdar SK, Kumashiro N, Petersen MC, Rahimi Y, Gattu AK, et al. Insulin-independent regulation of hepatic triglyceride synthesis by fatty acids. Proc Natl Acad Sci U S A 2015;112:1143-1148.
19) Goedeke L, Rotllan N, Canfran-Duque A, Aranda JF, Ramirez CM, Araldi E, et al. MicroRNA-148a regulates LDL receptor and ABCA1 expression to control circulating lipoprotein levels. Nat Med 2015;21:1280-1289.
20) Perry RJ, Peng L, Cline GW, Butrico GM, Wang Y, Zhang XM, et al. Non-invasive assessment of hepatic mitochondrial metabolism by positional isotopomer NMR tracer analysis (PINTA). Nat Commun 2017;8:798.
21) Camporez JP, Kanda S, Petersen MC, Jornayvaz FR, Samuel VT, Bhanot S, et al. ApoA5 knockdown improves whole-body insulin sensitivity in high-fat-fed mice by reducing ectopic lipid content. JLipid Res 2015;56:526-536.
22) Petersen MC, Madiraju AK, Gassaway BM, Marcel M, Nasiri AR, Butrico G, et al. Insulin receptor Thr1160 phosphorylation mediates lipid-induced hepatic insulin resistance. JClin Invest 2016;126:4361-4371.
23) Harriman G, Greenwood J, Bhat S, Huang X, Wang R, Paul D, et al. Acetyl-CoA carboxylase inhibition by ND-630 reduces hepatic steatosis, improves insulin sensitivity, and modulates dyslipidemia in rats. Proc Natl Acad Sci U S A 2016;113:E1796-E1805.
24) Blachnio-Zabielska AU, Chacinska M, Vendelbo MH, Zabielski P. The crucial role of C18-Cer in fat-induced skeletal muscle insulin resistance. Cell Physiol Biochem 2016;40:1207-1220.
25) Hla T, Kolesnick R. C16:0-ceramide signals insulin resistance. Cell Metab 2014;20:703-705.
26) Yuan G, Al-Shali KZ, Hegele RA. Hypertriglyceridemia: Its etiology, effects and treatment. CMAJ 2007;176:1113-1120.
27) Millar JS, Cromley DA, McCoy MG, Rader DJ, Billheimer JT. Determining hepatic triglyceride production in mice: comparison of poloxamer 407 with Triton WR-1339. JLipid Res 2005;46:2023-2028.
28) Merkel M, Eckel RH, Goldberg IJ. Lipoprotein lipase: genetics, lipid uptake, and regulation. JLipid Res 2002;43:1997-2006.
29) Horton JD, Goldstein JL, Brown MS. SREBPs: activators of the complete program of cholesterol and fatty acid synthesis in the liver. JClin Invest 2002;109:1125-1131.
30) Hertz R, Bishara-Shieban J, Bar-Tana J. Mode of action of peroxisome proliferators as hypolipidemic drugs. Suppression of apolipoprotein C-III. JBiol Chem 1995;270:13470-13475.
31) Inaba T, Matsuda M, Shimamura M, Takei N, Terasaka N, Ando Y, et al. Angiopoietin-like protein 3 mediates hypertriglyceridemia induced by the liver X receptor. JBiol Chem 2003;278:21344-21351.
32) Lee JY, Parks JS. ATP-binding cassette transporter AI and its role in HDL formation. Curr Opin Lipidol 2005;16:19-25.
33) Georgiadi A, Kersten S. Mechanisms of gene regulation by fatty acids. Adv Nutr 2012;3:127-134.
34) Bourbeau MP, Bartberger MD. Recent advances in the development of acetyl-CoA carboxylase (ACC) inhibitors for the treatment of metabolic disease. JMed Chem 2015;58:525-536.
35) Svensson RU, Parker SJ, Eichner LJ, Kolar MJ, Wallace M, Brun SN, et al. Inhibition of acetyl-CoA carboxylase suppresses fatty acid synthesis and tumor growth of non-small-cell lung cancer in preclinical models. Nat Med 2016;22:1108-1119.
36) Donnelly KL, Smith CI, Schwarzenberg SJ, Jessurun J, Boldt MD, Parks EJ. Sources of fatty acids stored in liver and secreted via lipoproteins in patients with nonalcoholic fatty liver disease. JClin Invest 2005;115:1343-1351.
37) Ou J, Tu H, Shan B, Luk A, DeBose-Boyd RA, Bashmakov Y, et al. Unsaturated fatty acids inhibit transcription of the sterol regulatory element-binding protein-1c (SREBP-1c) gene by antagonizing ligand-dependent activation of the LXR. Proc Natl Acad Sci U S A 2001;98:6027-6032.
38) Yoshikawa T, Shimano H, Yahagi N, Ide T, Amemiya-Kudo M, Matsuzaka T, et al. Polyunsaturated fatty acids suppress sterol regulatory element-binding protein 1c promoter activity by inhibition of liver X receptor (LXR) binding to LXR response elements. JBiol Chem 2002;277:1705-1711.
39) Hannah VC, Ou J, Luong A, Goldstein JL, Brown MS. Unsaturated fatty acids down-regulate srebp isoforms 1a and 1c by two mechanisms in HEK-293 cells. JBiol Chem 2001;276:4365-4372.
40) Moon YA, Liang G, Xie X, Frank-Kamenetsky M, Fitzgerald K, Koteliansky V, et al. The Scap/SREBP pathway is essential for developing diabetic fatty liver and carbohydrate-induced hypertriglyceridemia in animals. Cell Metab 2012;15:240-246.
41) Abu-Elheiga L, Matzuk MM, Abo-Hashema KA, Wakil SJ. Continuous fatty acid oxidation and reduced fat storage in mice lacking acetyl-CoA carboxylase 2. Science 2001;291:2613-2616.

Supporting Information

Additional Supporting Information may be found at onlinelibrary.wiley.com/doi/10.1002/hep.30097/suppinfo.